Interactions Crucial for Three-Dimensional Domain Swapping in the HP-RNase Variant PM8

Pere Tubert,[†] Douglas V. Laurents,[‡] Marc Ribó,[†] Marta Bruix,[‡] Maria Vilanova,[†*] and Antoni Benito[†*]
[†]Laboratori d'Enginyeria de Proteïnes, Departament de Biologia, Facultat de Ciències, Universitat de Girona, Campus de Montilivi, Maria Aurèlia Campmany, 69 E-17071 Girona, Spain and Institut d'Investigació Biomèdica de Girona (IdIBGi), Girona, Spain; and [‡]Instituto de Química Física "Rocasolano", Consejo Superior de Investigaciones Científicas, Serrano 119, E-28006 Madrid, Spain

ABSTRACT The structural determinants that are responsible for the formation of higher order associations of folded proteins remain unknown. We have investigated the role on the dimerization process of different residues of a domain-swapped dimer human pancreatic ribonuclease variant. This variant is a good model to study the dimerization and swapping processes because dimer and monomer forms interconvert, are easily isolated, and only one dimeric species is produced. Thus, simple models for the swapping process can be proposed. The dimerization (dissociation constant) and swapping propensity have been studied using different variants with changes in residues that belong to different putative molecular determinants of dimerization. Using NMR spectroscopy, we show that these mutations do not substantially alter the overall conformation and flexibility, but affect the residue level stability. Overall, the most critical residues for the swapping process are those of one subunit that interact with the hinge loop of another one-subunit residue, stabilizing it in a conformation that favors the interchange. Tyr^{25}, Gln^{101}, and Pro^{19}, with Asn^{17}, Ser^{21}, and Ser^{23}, are found to be the most significant; notably, Glu^{103} and Arg^{104}, which were postulated to form salt bridges that would stabilize the dimer, are not critical for dimerization.

INTRODUCTION

"Three-dimensional domain swapping" is a term used to describe the process that usually leads to the formation of an intertwined oligomer wherein two or more identical protein chains exchange the same structural element that is usually referred to as a "domain" (1). The swapped domain may correspond to an entire tertiary globular domain or simply to a single element of secondary structure (2) and usually is at the N- or C-terminus, although an internal domain has been described in at least one case (3). The exchangeable domain is usually appended to a flexible hinge region or loop and this hinge can swing to allow the swapped region to pack correctly in both the intramolecular and intermolecular structures. The resulting oligomers are composed of subunits that have the same structure as the original monomer, with the exception of this hinge loop.

The closed interface is the intramolecular interface found in the monomer structure that is recreated by two polypeptide chains in the domain-swapped structure. This interface constitutes the main adhesive force allowing the domain swapped oligomer to form. In a domain-swapped dimer, a new interface, the open interface, is formed when nonswapped regions of the subunits contact each other. When this interface is present, any favorable interactions found there stabilize the oligomeric state and compensate for the loss of entropy which is probably the main factor opposing oligomerization (4,5).

Different members of the pancreatic ribonuclease (RNase) family provide interesting models for the study of the transition from a monomer to a three-dimensional domain-swapped dimer. Bovine seminal RNase (BS-RNase) exists in nature as a dimer. The two subunits are crosslinked by two disulfide bonds between Cys^{31} of each chain and Cys^{32} of the other one (6). The dimer has the unique feature that it consists of an equilibrium mixture of two functionally active forms: one of which has swapped N-terminal domains (the M × M form) whereas the second one is not swapped (M = M) (7).

Unlike BS-RNase, other RNases, such as bovine pancreatic RNase (RNase A) and PM8, a human pancreatic RNase (HP-RNase) variant (8), are generally found as monomers, but they are able to form noncovalent domain swapped dimers in vitro (9,10), and the latter forms some dimer in vivo (11). These proteins share between 70 and 80% sequence identity and can swap the homologous N-terminal helix, although the resulting relative orientation of the subunits is different (for a review, see (12)). In addition, RNase A is the only known protein that can alternatively interchange a domain located at the C-terminus (2).

The crystal structure of PM8 is constituted by a new kind of N-terminal domain-swapped dimer (10). The oligomeric structure was unexpected because, in solution, most PM8 molecules exist as monomers. Nevertheless, the presence of a few dimers and oligomers was confirmed by nondenaturing electrophoresis (10) and by size-exclusion chromatography in the presence of 20% ethanol (13). Thus, the equilibrium between the monomer and dimer is displaced toward the monomer in aqueous solutions. The analysis of the structure indicated that the electrostatic interactions found along the open interface of the PM8 dimer were too weak to stabilize it in aqueous solution even at the highest protein concentration. These interactions could be more favored in the crystal

Submitted May 17, 2011, and accepted for publication June 13, 2011.

*Correspondence: antoni.benito@udg.edu or maria.vilanova@udg.edu

Editor: Patrick Loria.

0006-3495/11/07/0459/9 $2.00

doi: 10.1016/j.bpj.2011.06.013

due to the low dielectric constant of the precipitant solution and the high effective protein concentration.

We have proposed a model to explain the domain swapping process of PM8 (12,13). This model involves two steps: First, two monomers of PM8, which have a highly dynamic hinge loop, interact to produce an open interface. Second, after the formation of this new interface, additional residues of one monomer would interact with the hinge loop of the other monomer and stabilize it in an ordered conformation. (This conformational change would fix the highly dynamic stretch in a conformation that would promote the domain-swapping, and therefore, relative positions of the two subunits in the dimer would prepare the molecule for the interchange.)

In this work, we have characterized the molecular determinants contributing to three-dimensional domain swapping in this HP-RNase variant. Our results show that residues Gln^{101} and Tyr^{25} are very critical for the dimerization and the swapping process. In contrast, we show that Glu^{103} and Arg^{104}, which were postulated to form salt bridges that would stabilize the dimer, do not do so. Mutational analysis of the polar residues Asn^{17}, Ser^{21}, and Ser^{23} of the hinge loop reveals that their intermolecular hydrogen bonds contribute to domain swapping by modifying the dynamic behavior of the hinge loop.

MATERIALS AND METHODS

Construction of variants of PM8 and PM8E103C

Construction of PM8 and PM8E103C has been previously described in Canals et al. (10) and Rodríguez et al. (13). PM8 is an HP-RNase variant carrying five substitutions at the N-terminus: $Arg^{4}Ala$, $Lys^{6}Ala$, $Gln^{9}Glu$, and $Asp^{16}Gly$, and $Ser^{17}Asn$ together with the replacement $Pro^{101}Gln$. PM8E103C is a variant of PM8 carrying the substitution $Glu^{103}Cys$ and has been used to create covalent dimers of PM8 (13). Variants of PM8 and PM8E103C were constructed using the QuikChange kit (Stratagene, La Jolla, CA) following the manufacturer's instructions.

Ribonuclease expression and purification

HP-RNase variants were produced and purified essentially as described in Ribó et al. (14). The molecular mass of each variant was confirmed by matrix-assisted laser desorption/ionization-time of flight (MALDI-TOF) mass spectrometry using Bruker-Biflex (Bruker BioSpin, Billerica, MA) equipment in the Biocomputation and Protein Sequencing Facility of the Institut de Biotecnologia i Biomedicina of the Universitat Autònoma de Barcelona (Spain). In some cases, MALDI-TOF was also used to identify a glutathione moiety, probably to Cys^{103}.

The protein concentration of the variants was determined by UV spectroscopy using the extinction coefficients of 7,950 M^{-1} cm^{-1} and 16,025 M^{-1} cm^{-1} for monomers and covalent dimers, respectively, except for PM8_Y25A and PM8E103C_Y25A. For the latter variants, the extinction coefficients, 6,460 M^{-1} cm^{-1} and 13,045 M^{-1} cm^{-1} for monomers and covalent dimers, respectively, were calculated according to the method of Pace et al. (15).

Production of dimeric PM8E103C variants

Purified monomeric PM8E103C variants presented one moiety of glutathione bound to Cys^{103}. Each protein was dissolved in one ml of 100 mM Tris/acetate, 1.7 mM DTT, pH 8.5 (final monomer concentration 2.5 mg/ml) and incubated for 30 min at 25°C. In these conditions, only the intermolecular disulfide bond with glutathione is reduced. The dimer was then purified by size exclusion chromatography at a flow of 0.4 ml/min using a G75 HR 10/30 column (Amersham Biosciences, Piscataway, NJ) equilibrated with 200 mM sodium acetate pH 5.0 as described in Rodríguez et al. (13).

Production of labeled PM8E103C variants for NMR studies

The double uniformly labeled $^{13}C/^{15}N$ PM8E103C variant was produced following the protocol previously described. *Escherichia coli* BL21(DE3) cells were grown in a M9 minimal medium with $^{15}NH_4Cl$ (1 g/L) and $^{13}C_6$-glucose (4 g/L) (Cambridge Isotope Labs, Andover, MA) as sole nitrogen and carbon sources, respectively. Protein purification was achieved as described above for the nonlabeled variants. The purity of the protein samples was confirmed by MALDI_TOF analysis. Following a similar protocol using a M9 minimal medium with $^{15}NH_4Cl$ (1 g/L) as sole nitrogen source (Cambridge Isotope Labs), ^{15}N-labeled samples of PM8E103C_H80S and PM8E103C_3A variants were also produced. Labeled PM8E103C dimer was obtained as described above for the nonlabeled variants.

Assessment of the extent of the domain-swapping

The degree of N-terminal domain swapping was investigated in crosslinking experiments with divinyl sulfone (DVS) using the protocol described by Ciglic et al. (16). Briefly, PM8E103C (14 μg, 1 nM of subunit) in 100 mM sodium acetate, pH 5.0 (100 μL) and DVS (1 μL 10% solution in ethanol, 1 μM) were incubated at 30°C. This is an ~1000-fold excess of sulfone per subunit of the protein. Aliquots were withdrawn over a period of 150–250 h depending on the variant, and the reaction was quenched by adding 2-mercaptoethanol (final concentration 200 mM) and incubating for 15–30 min at room temperature. The samples were analyzed by reducing sodium dodecyl sulfate-polyacrylamide gel electrophoresis (SDS-PAGE) and bands were revealed by Coomassie Blue staining, and quantified by densitometry using the Quantity One software (Bio-Rad Laboratories, Hercules, CA).

NMR spectroscopy

Typically, NMR samples contained up to 0.5 mM of protein and were prepared in 90% H_2O/10% D_2O and D_2O at pH 4.5. All NMR spectra were recorded on a model No. AV-800 spectrometer (Bruker BioSpin) equipped with a cryoprobe at 25°C. For labeled $^{13}C/^{15}N$ PM8E103C monomer, assignment of ^{1}H, ^{13}C, and ^{15}N resonances was achieved using a standard suite of heteronuclear two-dimensional and triple resonance three-dimensional spectra: ^{1}H-^{15}N-heteronuclear single quantum coherence (HSQC), ^{1}H-^{13}C-HSQC, HN(CO)CA, HNCA, CBCA(CO)NH, CBCANH, and HNCO and a careful comparison with the reported assignment for wt-HP-RNase (Biological Magnetic Resonance Bank code: 4370). ^{1}H, and ^{15}N resonances of PM8E103C_H80S and PM8E103C_3A monomer variants were assigned by comparison with PM8E103C with the help of three-dimensional ^{1}H-^{15}N-HSQC-total correlation spectroscopy (TOCSY) and ^{1}H-^{15}N-HSQC-nuclear Overhauser enhancement spectroscopy (NOESY) spectra. The spectra of the dimeric form of PM8E103C were assigned by comparison with the corresponding monomer on the bases of three-dimensional ^{1}H-^{15}N-HSQC-NOESY experiment recorded in the same conditions.

NMR relaxation experiments were carried out at the same conditions described above. Conventional ^{15}N heteronuclear nuclear Overhauser effect (NOE) data were determined for the PM8E103C, PM8E103C_H80S, and

PM8E103C_3A monomeric variants. The experiments with and without proton saturation were acquired simultaneously in an interleaved manner with a recycling delay of 5 s, and were split during processing into separate spectra for analysis. The values for the heteronuclear NOEs were obtained from the ratio intensities of the resonances according to I_{sat}/I_{ref}. The uncertainty was estimated to be ~5%.

Finally, NMR was also used to study the conformational stability on the residue level by hydrogen-deuterium exchange experiments with PM8E103C, PM8E103C_3A, and PM8E103C_H80S variants. The exchange of amide protons with solvent deuterons was started by dissolving lyophilized, protonated ^{15}N variant samples into deuterated solvent. The temperature and pH* values of the exchange experiments were the same as those used in the assignment process (see above). The hydrogen exchange rates were determined by integrating the volume of ^{1}H-^{15}N amide crosspeaks in a series of heteronuclear single quantum coherence (HSQC) spectra recorded consecutively after a dead time of ~30 min. A single-exponential decay function was fit to the data to determine the observed exchange rate, k_{ex}. The intrinsic exchange rates for unprotected HN groups, k_{rc}, were calculated using the parameters reported by Bai et al. (17) corrected for pH* 4.5 and temperature. Using equations described therein, the protection factors, i.e., the ratio of the intrinsic and observed exchange rates, of the individual groups were determined. When exchange is governed by the EX2 regime, as commonly occurs for RNases under similar conditions of temperature and pH (18,19), the conformational stability, ΔG_{HX}, of each amide group can be calculated from the protection factor

$$\Delta G_{HX} = -RT \ln(k_{ex}/k_{rc}) = -RT \ln K_{op} = -RT \ln(1/PF),$$

where K_{op} is the local or global equilibrium constant for the opening reaction and *PF* the protection factor. Spectra were processed with Topspin (Bruker BioSpin, Karlsruhe, Germany) and analyzed and integrated with SPARKY (T. D. Goddard and D. G. Kneller, SPARKY, University of California at San Francisco, San Francisco, CA).

Kinetics of dimerization of PM8 variants and K_d calculations

Monomeric PM8 variants were incubated at 29°C in 50 mM MOPS (3-(*n*-morpholino)propanesulfonic acid), 50 mM NaCl, and 20% ethanol, pH 6.7 at concentrations ranging from 0.1 to 1.5 mM. After 100 h of incubation, aliquots were withdrawn, and the mixtures were immediately chromatographed at a flow rate of 0.4 ml/min on a Sephadex G75 HR 10/30 column (Pharmacia, GE Lifesciences, Waukesha, WI). Because no protein aggregation or higher oligomers were observed in these experiments, the concentrations of monomer and dimer could be quantified by integrating their peaks. Only when the samples reached equilibrium were they were used for K_d calculations. Given the equilibrium $M + M \leftrightarrow D$, the K_d can be calculated from the slope of a plot of M^2 concentration versus D concentration (13,20). The dimer was rechromatographed immediately after the recovery of the peak at 72 h later, and the amount of RNase reeluted as a dimer was of 100% and 70%, respectively (not shown). This indicated that the exchange between dimer and monomer was slow on the timescale of the chromatography.

Determination of thermal stability

The conformational stability of the different variants was determined by circular dichroism (CD). CD spectra were recorded using a J-810 spectropolarimeter (JASCO, Oklahoma City, OK) equipped with a thermostated cell holder. The protein was dissolved at 20 μM in 100 mM KH_2PO_4 10% D_2O. A quartz cell of 0.2-cm optical pathlength was used to record the molar ellipticity (E_m) at 218 nm. The temperature was raised from 20 to 85°C and the signal was recorded at 0.5°C. The solvent contribution was subtracted using KaleidaGraph software (Synergy Software, Bangkok, Thailand). Temperature-unfolding transitions curves were fitted to a two-state thermodynamic model combined with sloping linear functions for the native and denatured states, as described elsewhere (21).

RESULTS

Protein design

To characterize their role on the three-dimensional domain swapping and dimerization of PM8, we replaced by site-directed mutagenesis different residues of this RNase. Three kinds of variants were envisaged, as follows.

Variants to study the role of residues postulated to be important for forming the initial open interface

In the crystal structure of PM8 (10), the open interface is mainly stabilized by two electrostatic interactions between residues Arg^{104} and Glu^{103} of both subunits (Fig. 1 *A*). To test the possibility that residues Arg^{104} and Glu^{103} were important for the formation of the nascent nonswapped PM8 dimer, we constructed a PM8_E103S_R104S variant in which both charged residues were replaced by Ser. These Ser residues are too far apart at the interface to establish interchain hydrogen bonds, and we have not detected other alternative interactions in the PM8 structure.

Variants to study the role in the dimerization and on the domain swapping of residues postulated to interact with the hinge loop of the other subunit, stabilizing it in a conformation that favors the interchange

In the structure of the PM8 dimer, the side chains of Gln^{101} and Tyr^{25} of each subunit create a cavity in which the Pro^{19} of the other subunit is sandwiched (Fig. 1 *B*), fixing the hinge loop in a conformation that extents to the other subunit (10). In addition, Gln^{101} establishes three hydrogen bonds with the Ser^{20} residues from both subunits which further stabilize the extended conformation of the hinge loop in the dimer. To study the role of these two residues on the dimerization and on the domain-swapping process, we constructed variants of PM8 in which Gln^{101} and Tyr^{25} were substituted by Ala (variants PM8_Q101A and PM8_Y25A, respectively).

Variants to study the role of the hinge loop stability on dimerization

We previously postulated that the stability of the hinge loop upon dimerization could be very important in determining the propensity of the dimer to swap (13). Analysis of the crystal structure of dimeric PM8 (10) reveals the presence of a hydrogen-bond network within the hinge loop that stabilizes this stretch on a helix 3_{10} conformation and that is absent in a closely related monomeric variant (PM7 (22)). We have studied the effect of removing specific side-chain-sidechain hydrogen bonds inside the hinge loop that stabilize this stretch in a 3_{10} helical conformation (Fig. 1 *C*),

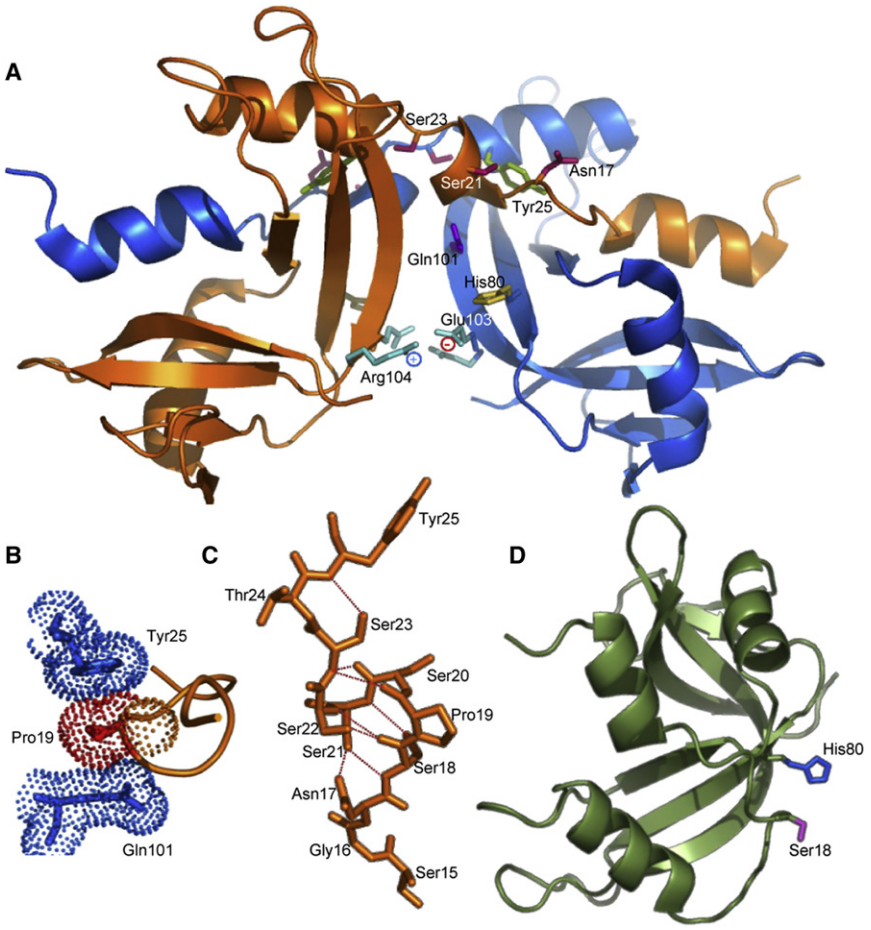

FIGURE 1 Details of the molecular determinants investigated in the PM8 dimer. (*A*) General view of the dimeric structure of PM8. Residues modified in this work are indicated in only one of the two subunits. One of the two electrostatic interactions found between Glu^{103} and Arg^{104} is also indicated by minus and plus signs. (*B*) Detail of the stacking between Pro^{19} (*red*) from one subunit with Tyr^{25} and Gln^{101} (*blue*) from the other subunit in the dimeric structure of PM8. The van der Waals surfaces of these residues are shown as dotted surfaces. (*C*) Stabilization of the hinge loop in a helical conformation by multiple-centered hydrogen bonds (*discontinuous red lines*) belonging to the same chain residues. (*D*) General view of the PM7 human pancreatic RNase monomeric variant (Protein DataBank accession code: 1DZA). The residues 1, 18–22, and 126–128 were not solved in the crystal structure and have been modeled (22). The figure was drawn using the software PyMol (DeLano Scientific, http://www.pymol.sourceforge.net/).

which is present only in the dimer. We selected residues Asn^{17}, Ser^{21}, and Ser^{23} to create variants PM8_3A.

Additionally, in an attempt to stabilize the hinge peptide of monomeric PM8, we took advantage of previous results with BS-RNase and RNase A to design a variant that could possess a less dynamic hinge loop. It has been described that the hinge loop of RNase A is mainly stabilized by a hydrogen bond established only in the monomer between Ser^{18} and Ser^{80} and that the substitution of Ser^{80} by Arg produces a variant with a highly dynamic hinge peptide (23). Furthermore, it has been shown for hA-mBS (a monomeric BS-RNase variant in which the hinge peptide sequence has been substituted by that of RNase A, together with the replacement of Asn^{67} by Asp) that the substitution of Arg^{80} by Ser reduces both the flexibility of the hinge peptide region and the swapping propensity from 70% to 30% (24).

The decrease in swapping propensity was attributed to the gain of a stabilizing interaction between Ser^{80} and Ser^{18} in the monomeric form (24) and to the loss of favorable interactions afforded by this positive charge in the dimer (25). We postulated that replacing His^{80} by Ser in PM8 could allow the formation of a hydrogen bond between Ser^{18} and the incorporated Ser^{80}, resulting in a stabilization of the hinge peptide in the monomer (Fig. 1 *D*). Consequently, we constructed a variant of PM8 in which His^{80} was substituted by Ser (variant PM8_H80S) to study the effect that this mutation has on dimerization and domain swapping. Different replacements performed in each variant can be found in Table S1 in the Supporting Material.

Assessment of the global fold

Before performing the dimerization studies, the structure of some variants used in this work was characterized by NMR. To begin, the ^{1}H, ^{15}N, and ^{13}C NMR spectral resonances of PM8E103C were assigned by following the three-dimensional strategy (26) and the conformational chemical shifts ($\Delta\delta = \delta_{\text{experimental}} - \delta_{\text{random coil}}$) for C$\alpha$ and Cβ nuclei are represented in Fig. 2. The analysis of these data confirms that this variant is correctly folded and has the expected secondary structure.

The NMR spectra of the monomeric variants, PM8E103C_H80S and PM8E103C_3A, and of the PM8E103C dimer, were assigned by comparison with those of the monomeric PM8E103C. Because chemical shifts are

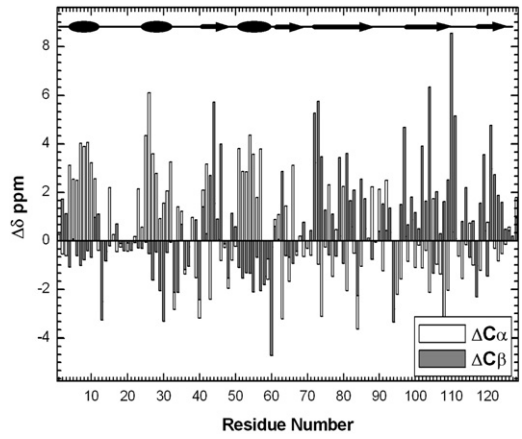

FIGURE 2 NMR conformational chemical shifts ($\Delta\delta$, ppm) for the $^{13}C\alpha$ and $^{13}C\beta$ nuclei of PM8E103C variant. (*Top*) Secondary structural elements: α-helices (*ellipses*) and β-sheets (*arrows*).

very sensitive to conformational changes, they were used to monitor the effects of mutations and PM8E103C dimerization on structure (see Fig. S1 in the Supporting Material). Comparing the PM8E103C monomer and dimer, large changes in the chemical shifts are observed in the hinge loop which reflects the transformation of its structure upon dimerization. Much smaller but significant $\Delta\delta$ values are observed in the loops and segments (residues 48–49, 80–83, and 101–103) that form the open interface (Fig. 3 *A*). Remarkably, helix 1, the swapped structural element, shows essentially identical δ-values in the monomer as compared to the dimer, indicating that its conformation and environment are practically unchanged.

In the case of the PM8E103C_3A variant, the three substitutions introduced in the hinge loop lead to very large chemical shift differences in this loop; in fact, one ^{15}N signal changes over 4 ppm and three other peaks are altered by >1 ppm (see Fig. S1 *B*). Moreover, changes of 0.2–0.6 ppm are seen in segments 48–49, 80–82, and 101–102. This pattern of important differences is also observed in the ^{1}H nucleus. In the variant PM8E103C_H80S, large displacements in ^{15}N, >1 ppm, are seen both at the site of the substitution and in residues 101–103 at the open interface, which is nearby in the structure (see Fig. S1 *C*). Smaller but still important changes in ^{15}N are observed in loops 14–23 and 48–49. The chemical shift changes in ^{1}H are notable, being >0.05 ppm in the abovementioned residues; there are also more-minor changes in other parts of the protein.

Among all these variants, the chemical shifts are very similar in the loops composed of residues 34–42, 64–70, 87–96, and 112–114, which is evidence of an absence of substantial conformational differences. All these loops are located far from the hinge loop and open interface. Moreover, the structure of the most of the elements of secondary structure is essentially the same in the different variants (as gauged by the chemical shift differences) except the

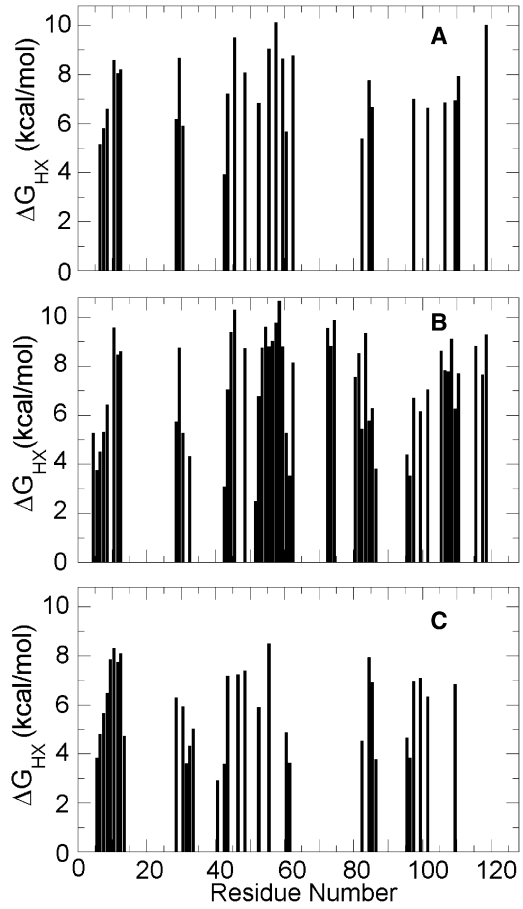

FIGURE 3 Conformational free energies (in kcal/mol) of individual amide hydrogens in PM8E103C (*A*), PM8E103C_3A (*B*), and PM8E103C_H80S (*C*) measured by NMR-monitored hydrogen exchange at 25°C, pH* 4.5.

β-strands composed of residues 79–86 and 97–111, which participate in the formation of the open interface. Based on the chemical-shift differences, it can be concluded that the overall backbone structure and native fold is generally conserved in these variants and that the large structural changes are confined to the hinge loop and open interface (see Fig. S1).

We assessed whether or not the introduction of the different mutations had altered their stability by characterizing the temperature-unfolding process of PM8E103C variants and determining their midpoint denaturation temperatures ($T_{1/2}$) (Table 1). In all cases only one transition was observed (not shown). The $T_{1/2}$ of most of the variants differed only in 1–2°C relative to PM8E103C. For PM8E103C_Y25A, the $T_{1/2}$ is ~7°C lower. This large stability decrease can be attributed to the loss of hydrophobic and van der Waals interactions and a Tyr^{25}-OH -$^{-}$OOC-Asp^{14} hydrogen bond (27).

For comparison, conformational stability of PM8E103C, PM8E103C_3A, and PM8E103C_H80S was also measured

TABLE 1 Biophysical characterization of the different HP-RNase variants analyzed

PM8 variant	Structural determinant tested	$T_{1/2}$ (°C)*	$\Delta G°_{HX}$† (kcal/mol)	K_d‡ (mM)	Amount swapped
PM8	Pseudo wild-type.	55.4¶	ND	7.4/12.5§	100%
PM8E103C	Induces covalent dimer.	61.8	9.9	Covalent dimer	100%
PM8_3A	H-bonds in swapped hinge loop on dimerization.	ND	ND	$>10^4$‖	ND
PM8E103C_3A	H-bonds in hinge loop on swapping.	62.6	10.3	Covalent dimer	50%
PM8_Y25A	Y25, P19 ring stacking on dimerization.	ND	ND	$>10^4$‖	ND
PM8E103C_Y25A	Y25, P19 ring stacking on swapping.	54.8	ND	Covalent dimer	0%
PM8_Q101A	H-bonds to S20, P19 packing on dimerization.	ND	ND	$>10^4$‖	ND
PM8E103C_Q101A	H-bonds to S20, P19 packing on swapping.	61.1	ND	Covalent dimer	55%
PM8_H80S	H-bond to hinge loop on dimerization.	ND	ND	0.50	ND
PM8E103C_H80S	H-bond to hinge loop on swapping.	60.0	8.3	Covalent dimer	100%
PM8_E103S_R104S	Salt bridges at open interface on dimerization.	60.0	ND	4.5	ND

ND, not determined.

*Values for monomeric forms calculated from temperature denaturation curves followed by CD. Experimental uncertainty: 0.1–0.4°C.

†Values for monomeric forms calculated from hydrogen exchange experiments by NMR. Experimental uncertainty: 0.2 kcal/mol.

‡Values calculated from the slope of a plot of M^2 concentration versus D concentration. Experimental uncertainty: 0.04 mM (H80S), 0.4–0.7 mM (other variants).

§Value calculated at pH 8.0. All the other K_d values were calculated at pH 5.0.

¶Data from Canals et al. (8).

‖K_d limit calculated based on the minimal amount of dimer detectable during chromatographic analysis.

by hydrogen exchange (Fig. 3 and Table 1) (28). For PM8E103C_3A, this value is 10.3 kcal/mol, slightly larger than the value obtained for PM8E103C, 9.9 kcal/mol, which is in line with the rank order of the stabilities defined by thermal denaturation. On the other hand, the internal dynamics as measured by the ^{15}N-^{1}H NOE shows that the NOE ratio, which gauges the backbone flexibility on the picosecond-to-nanosecond timescale, is very similar to the other variants as shown in Fig. S2.

For PM8E103C_H80S, the conformational stability measured by hydrogen exchange is slightly reduced (Table 1). Interestingly, the decrease in the conformational stability shows variation on the level of individual residues (Fig. 3). All the secondary structural elements are less stable than in the other variants, except for the first α-helix, which is the most stable element of structure in this variant. Taken together, the data indicate that the mutations do not dramatically decrease the variant's global stability.

Effects on the propensity to swap

The degree of swapping was investigated by crosslinking His^{12} and His^{119} with divinyl sulfone (DVS) (16), which crosslinks both of the active site His. If the active site of the dimer is composite, with His^{12} coming from one subunit and His^{119} coming from the other, the crosslink should covalently join the two subunits, which remain bound even under reducing conditions. Otherwise, crosslinking connects two His from the same subunit, yielding monomers under reducing conditions. Because the disposition of both His residues is equal in monomeric and composite active sites, the reaction rates with DVS are equivalent in both cases. Determination of the swapping propensity of PM8 has the limitation that the formation of the open interface and the process of swapping both occur simultaneously, which makes it difficult to tweeze apart the interactions that govern these processes.

To overcome this limitation, we previously constructed a PM8 variant in which Glu^{103} was replaced by a Cys (13) to stabilize the open interface of the dimer by means of a disulfide bond (variant PM8E103C). This position was chosen because in the structure of the PM8 dimer (10) the Cα atoms of the two Glu^{103} side chains are facing each other (Fig. 1) and are separated by a distance similar to that found between the equivalent atoms of two Cys in longer disulfide bonds. Because dissociation does not occur in this variant dimer, we could specifically study its degree of swapping. We took advantage of this variant to construct a new set of variants designed to investigate the role of the residues described above on the domain-swapping process. Variants were PM8E103C_Y25A, in which Tyr^{25} was substituted by Ala; PM8E103C_Q101A, in which Gln^{101} was substituted by Ala; PM8E103C_3A, in which Asn^{17}, Ser^{21}, and Ser^{23} were substituted by Ala; and PM8E103C_H80S in which His^{80} was substituted by Ser.

Different incubation times with DVS were assayed to optimize the reaction. After 150 h of incubation, the proportion of dimer and monomer in a reductive SDS-PAGE remained unchanged for all the variants, save PM8E103C_H80S (Fig. 4), indicating that the reaction was completed. The proportion of swapped molecules at equilibrium is shown in Table 1. In agreement with previous results (13), all the subunits of dimeric PM8E103C swapped the N-terminal α-helix. For PM8E103C_Q101A, a clear decrease of 50% relative to that of the parental variant in the swapping propensity was observed. A more drastic effect was observed for PM8E103C_Y25A in which no swapping could be detected. Interestingly, the swapping propensity of PM8E103C_3A decreased to one-half that of the parental variant and the replacement of His^{80} by

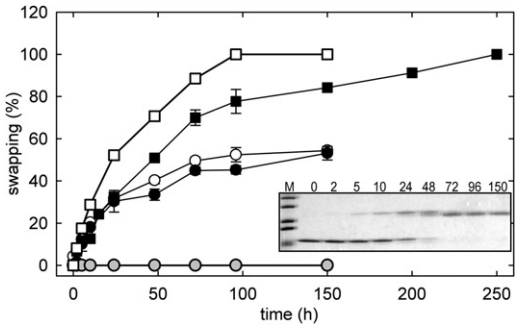

FIGURE 4 Degree of swapping in PM8E103C variants. PM8E103C (*open squares*), PM8E103C_H80S (*solid squares*), PM8E103_Y25A (*shaded circles*), PM8E103C_Q101A (*solid circles*), and PM8E103C_3A (*open circles*). Percentages shown in Table 1 were obtained when the reaction reached the equilibrium. (*Inset*) SDS-PAGE analysis of the DVS cross-linking reaction for PM8E103C. Incubations times (*h*) are indicated over each lane. Molecular mass markers correspond to 15, 20, 25, 37, and 50 kDa.

Ser affected neither the propensity of the resulting variant to swap its N-terminal domain (Table 1) or the backbone flexibility of the hinge loop (see Fig. S2).

Effects on the K_d of the dimers

We also sought to analyze which of the replacements introduced in PM8 altered the propensity of the resulting variants to dimerize. The amount of dimer and monomer at equilibrium was measured from the areas of the corresponding peaks in molecular exchange chromatograms. For variants PM8_Q101A, PM8_Y25A, and PM8_3A, no dimer could be detected even at the highest concentrations assayed (Table 1). Taking into account an extinction coefficient of 13,045 M^{-1} cm^{-1} for PM8_Y25A, of 13,045 M^{-1} cm^{-1} for PM8_3A, and of 15,900 M^{-1} cm^{-1} for PM8_Q101A for these variants, considering the highest protein concentration used (1.5 mM) and that the lower detection threshold of the dimer peak in the HPLC is 1 mAU, the estimated lower limit on the K_d value is >36 M for PM8_Y25A and PM8_3A, and >29 M for PM8_Q101A.

These mutations produce a 10^3-fold increase of the K_d compared to the parental variant (see Table 1), which corresponds to a free energy difference of roughly 5 kcal/mol. This value has been estimated at 29°C, the temperature at which the K_d values have been calculated. The K_d of PM8_H80S is significantly lower compared to that of PM8 (Table 1), thus the PM8_H80S dimer is more stable. Notably, the PM8 dimer is somewhat less stable at pH 8.0, where His^{80} is mainly neutral as compared to pH 5.0 where His^{80} is chiefly in the charged state (Table 1). This suggests that the stabilization of the dimer by the His^{80} to Ser substitution is not due to the removal of the positive charge of His^{80}. Finally, we found that the replacement of Glu^{103} and Arg^{104} by Ser decreases the K_d of the resulting dimer (Table 1) (that is, it makes the dimer slightly more stable).

DISCUSSION

In contrast to RNase A which must unfold to attain a domain-swapped dimer (29), the PM8 and BS-RNase can interchange its N-terminal domains while maintaining the native structure in solution. Site-directed mutagenesis has allowed us to investigate the role of different residues in both the swapping and dimerization of PM8. The analysis of the structure, dynamics, and conformational stability of the variants have provided evidence that the mutations introduced in this work do not significantly affect the stability and overall tertiary structure, although considerable effects on the conformation of segments near the mutated site are observed. These results are not surprising because the tertiary structure is preserved even in more severely destabilized RNase A variants in which structural changes are limited to the neighborhood of the mutation site (18,30).

Concerning the early events of the PM8 dimerization when the swapping event has not still occurred, the relative positions of the subunits would prepare the molecule for the swapping of the N-terminal domains. Because charge-charge interactions act over long distances, it was feasible that favorable electrostatic interactions between Glu^{103} and Arg^{104} from different monomers (that are also found in the swapped dimer (Fig. 1 *A*)) aid the approach and correct orientation of the monomers during the earliest stages of dimerization. Nevertheless, here we have shown by substituting Glu^{103} and Arg^{104} by Ser that their electrostatic interactions are not critical to form this initial dimer. Afterwards, the side chain of Arg^{104}, which is mobile and samples a wide variety of conformations in HP-RNase monomer (31), would necessarily become fixed and lose conformational entropy to adopt the fixed, salt-bridged structure seen in the PM8 crystal structure. The observed K_d value for the PM8_E103S_R104S variant may suggest that this unfavorable loss of conformational entropy may slightly outweigh the favorable contribution of the charge-charge interactions. It is possible that, in the inchoate noncovalent dimer, alternative open interfaces could form upon the removal of these charges residues from which domain-swapping could be produced. Accordingly, very different open interfaces have been described for highly related BS-RNase variants (32).

Regarding the role of residues Gln^{101} and Tyr^{25}, our results show that hydrogen bonds established by Gln^{101} and, more crucially, the sandwiching of the Pro^{19} ring between the Gln^{101} side chain and the Tyr^{25} ring, play a vital role in the stabilization of the hinge loop in its swapped conformation and on the capacity of the molecule to dimerize. Our results indicate that for PM8 these interactions are established by residues Gln^{101} and Tyr^{25}, which produce a more fixed conformation of the hinge loop that could help to drive the process of swapping. These findings are consistent with previous structural evidence (10,22) and results from the noncovalent and covalent swapped dimers

of BS-RNase in which Pro^{19} is also clamped between the side chains of residues Tyr^{25} and Gln^{101} (33–35), suggesting that this interaction may be also an important determinant for BS-RNase domain swapping.

We previously postulated that the propensity of swapping could depend on the relative stability of the hinge loop conformations in the monomer and dimers (12). For RNase A, the dynamic behavior of the hinge loop is restrained by different hydrogen bonds, but this is not the case for either BS-RNase or PM8. For RNase A, the restricted mobility of the hinge loop could explain why more severely destabilizing conditions are needed to form RNase A N-dimers. The importance of the hinge loop stability differences between monomeric and dimeric forms on swapping is highlighted by the yield of swapped molecules of the covalent dimeric RNase variants CC-RNase A (RNase A carrying Cys residues at position 31 and 32) (36), where BS-RNase and PM8E103C is compared. The former variant forms only low amounts of swapped molecules (15%) (25). On the other hand, the BS-RNase and the PM8E103C HP-RNase dimers are 70% and ~100% of swapped, respectively. The difference of the swapping efficiency between the human variant and BS-RNase has been attributed to a major stabilization of the hinge loop in the human variant (12). Therefore, we focused our interest to determine the effect of replacing Ser^{17}, Ser^{21}, and Ser^{23} by Ala.

In the case of PM8E103C_3A, removal of the polar residues that form intramolecular hydrogen bonds within the hinge loop in dimeric form of PM8 leads to a weaker dimer with less swapping. Interestingly, the hydrogen exchange measurements reveal that the stability differences are not uniform along the sequence. The stability of the first α-helix is highest in the PM8E103C_3A variant, with respect to PM8E103C, which might reflect the introduction of three Ala residues in the nearby hinge loop as Ala has the highest intrinsic helix-forming propensity (37). This confirms the hypothesis that this network of hydrogen bonds stabilizes the swapped, dimeric conformation of this loop (10). This variant is more stable than the parental PM8 and it is possible to advance the idea that this might be related to an increase of stability of the hinge loop in the monomeric form. The K_d experiments also reinforce the importance of these positions together with Tyr^{25} and Gln^{101} on the dimerization process. In all these cases, the mutations produce a 10^3-fold increase of the K_d compared to the parental variant, which corresponds roughly to a difference in free energy of 5 kcal/mol.

Regarding the role of His^{80}, it was expected that the $His^{80}Ser$ mutation might stabilize the monomer relative to the dimer, and to increase the fraction of monomer. Surprisingly, our results show that the PM8_H80S dimer is significantly stabilized, i.e., its K_d is lower. The comparison of the stability of individual amide hydrogens (Fig. 3) and backbone dynamics (see Fig. S2) between the hinge loop of monomeric PM8E103C and PM8E103C_H80S indicates that in this case the introduction of Ser^{80} does not alter the dynamic behavior of the hinge loop. We have also shown that the increase of dimer stability cannot be attributed to the removal of the positive charge of His that could be establishing unfavorable interactions with residues of the other monomer (i.e., repulsive charge-charge interactions). His^{80} protrudes somewhat from the open interface (Fig. 1 *A*) and it would be feasible that the removal of this residue could produce a new and more stable open interface. In fact, for PM8E103C_H80S, the larger displacement of ^{15}N and ^{1}H chemical shifts (see Fig. S1 *C*) were observed in residues located at the open interface (Gln^{101} to Cys^{103}) together with the site of the substitution, favoring the hypothesis of a local rearrangement of this region.

CONCLUSION

The results presented in this work indicate that the most critical residues involved in the dimerization process of PM8 are Tyr^{25} and Gln^{101} which interact with the Pro^{19} residue of the hinge loop of the other subunit. They also indicate that different primary open interfaces can lead to the formation of a swapped structure. Finally, it is derived that the predisposition to swap of a protein domain can be modulated by changing the stability of the hinge loop structures in the monomer or dimer.

Overall, this work gives clues for understanding the formation of oligomers in other proteins through three-dimensional domain swapping.

SUPPORTING MATERIAL

Two figures and one table are available at http://www.biophysj.org/biophysj/supplemental/S0006-3495(11)00710-7.

P.T. acknowledges his fellowship from Ministerio de Educación y Ciencia, Spain. Work was supported by grants No. BFU2009-06935/BMC, No. CTQ2010-21567-C02-02, and No. CTQ2008-00080/BQU from Ministerio de Ciencia e Innovación (Spain).

REFERENCES

1. Bennett, M. J., M. P. Schlunegger, and D. Eisenberg. 1995. 3D domain swapping: a mechanism for oligomer assembly. *Protein Sci.* 4:2455–2468.
2. Liu, Y., and D. Eisenberg. 2002. 3D domain swapping: as domains continue to swap. *Protein Sci.* 11:1285–1299.
3. Mizuno, H., Z. Fujimoto, …, T. Morita. 1997. Structure of coagulation factors IX/X-binding protein, a heterodimer of C-type lectin domains. *Nat. Struct. Biol.* 4:438–441.
4. Tamura, A., and P. L. Privalov. 1997. The entropy cost of protein association. *J. Mol. Biol.* 273:1048–1060.
5. Erickson, H. P. 1989. Co-operativity in protein-protein association. The structure and stability of the actin filament. *J. Mol. Biol.* 206:465–474.
6. Mazzarella, L., S. Capasso, …, A. Zagari. 1993. Bovine seminal ribonuclease: structure at 1.9 Å resolution. *Acta Crystallogr. D Biol. Crystallogr.* 49:389–402.

7. Piccoli, R., M. Tamburrini, …, G. D'Alessio. 1992. The dual-mode quaternary structure of seminal RNase. *Proc. Natl. Acad. Sci. USA.* 89:1870–1874.
8. Canals, A., M. Ribó, …, M. Vilanova. 1999. Production of engineered human pancreatic ribonucleases, solving expression and purification problems, and enhancing thermostability. *Protein Expr. Purif.* 17:169–181.
9. Crestfield, A. M., W. H. Stein, and S. Moore. 1963. On the preparation of bovine pancreatic ribonuclease A. *J. Biol. Chem.* 238:618–621.
10. Canals, A., J. Pous, …, M. Coll. 2001. The structure of an engineered domain-swapped ribonuclease dimer and its implications for the evolution of proteins toward oligomerization. *Structure.* 9:967–976.
11. Geiger, R., M. Gautschi, …, A. Helenius. 2011. Folding, quality control, and secretion of pancreatic ribonuclease in live cells. *J. Biol. Chem.* 286:5813–5822.
12. Benito, A., D. V. Laurents, …, M. Vilanova. 2008. The structural determinants that lead to the formation of particular oligomeric structures in the pancreatic-type ribonuclease family. *Curr. Protein Pept. Sci.* 9: 370–393.
13. Rodríguez, M., A. Benito, …, M. Vilanova. 2006. Characterization of the dimerization process of a domain-swapped dimeric variant of human pancreatic ribonuclease. *FEBS J.* 273:1166–1176.
14. Ribó, M., A. Benito, …, M. Vilanova. 2001. Purification of engineered human pancreatic ribonuclease. *Methods Enzymol.* 341:221–234.
15. Pace, C. N., F. Vajdos, …, T. Gray. 1995. How to measure and predict the molar absorption coefficient of a protein. *Protein Sci.* 4:2411–2423.
16. Ciglic, M. I., P. J. Jackson, …, S. A. Benner. 1998. Origin of dimeric structure in the ribonuclease superfamily. *Biochemistry.* 37:4008–4022.
17. Bai, Y., J. S. Milne, …, S. W. Englander. 1993. Primary structure effects on peptide group hydrogen exchange. *Proteins.* 17:75–86.
18. Bruix, M., M. Ribó, …, M. Vilanova. 2008. Destabilizing mutations alter the hydrogen exchange mechanism in ribonuclease A. *Biophys. J.* 94:2297–2305.
19. Qu, Y., and D. W. Bolen. 2003. Hydrogen exchange kinetics of RNase A and the urea:TMAO paradigm. *Biochemistry.* 42:5837–5849.
20. Russo, N., A. Antignani, and G. D'Alessio. 2000. In vitro evolution of a dimeric variant of human pancreatic ribonuclease. *Biochemistry.* 39:3585–3591.
21. Mozhaev, V. V., K. Heremans, …, C. Balny. 1996. High pressure effects on protein structure and function. *Proteins.* 24:81–91.
22. Pous, J., A. Canals, …, M. Coll. 2000. Three-dimensional structure of a human pancreatic ribonuclease variant, a step forward in the design of cytotoxic ribonucleases. *J. Mol. Biol.* 303:49–60.
23. Vatzaki, E. H., S. C. Allen, …, K. R. Acharya. 1999. Crystal structure of a hybrid between ribonuclease A and bovine seminal ribonuclease—the basic surface, at 2.0 Å resolution. *Eur. J. Biochem.* 260:176–182.
24. Ercole, C., R. Spadaccini, …, D. Picone. 2007. A new mutant of bovine seminal ribonuclease with a reversed swapping propensity. *Biochemistry.* 46:2227–2232.
25. Ercole, C., R. A. Colamarino, …, D. Picone. 2009. Comparison of the structural and functional properties of RNase A and BS-RNase: a stepwise mutagenesis approach. *Biopolymers.* 91:1009–1017.
26. Bax, A. 1994. Multidimensional nuclear magnetic resonance methods for protein studies. *Curr. Opin. Struct. Biol.* 4:738–744.
27. Juminaga, D., W. J. Wedemeyer, …, H. A. Scheraga. 1997. Tyrosyl interactions in the folding and unfolding of bovine pancreatic ribonuclease A: a study of tyrosine-to-phenylalanine mutants. *Biochemistry.* 36:10131–10145.
28. Huyghues-Despointes, B. M., J. M. Scholtz, and C. N. Pace. 1999. Protein conformational stabilities can be determined from hydrogen exchange rates. *Nat. Struct. Biol.* 6:910–912.
29. López-Alonso, J. P., M. Bruix, …, D. V. Laurents. 2010. NMR spectroscopy reveals that RNase A is chiefly denatured in 40% acetic acid: implications for oligomer formation by 3D domain swapping. *J. Am. Chem. Soc.* 132:1621–1630.
30. Kurpiewska, K., J. Font, …, K. Lewiński. 2009. X-ray crystallographic studies of RNase A variants engineered at the most destabilizing positions of the main hydrophobic core: further insight into protein stability. *Proteins.* 77:658–669.
31. Kövér, K. E., M. Bruix, …, M. Rico. 2008. The solution structure and dynamics of human pancreatic ribonuclease determined by NMR spectroscopy provide insight into its remarkable biological activities and inhibition. *J. Mol. Biol.* 379:953–965.
32. Merlino, A., C. Ercole, …, F. Sica. 2008. The buried diversity of bovine seminal ribonuclease: shape and cytotoxicity of the swapped non-covalent form of the enzyme. *J. Mol. Biol.* 376:427–437.
33. Merlino, A., L. Vitagliano, …, L. Mazzarella. 2004. Population shift vs induced fit: the case of bovine seminal ribonuclease swapping dimer. *Biopolymers.* 73:689–695.
34. Sica, F., A. Di Fiore, …, L. Mazzarella. 2004. Structure and stability of the non-covalent swapped dimer of bovine seminal ribonuclease: an enzyme tailored to evade ribonuclease protein inhibitor. *J. Biol. Chem.* 279:36753–36760.
35. Merlino, A., I. Russo Krauss, …, F. Sica. 2009. Toward an antitumor form of bovine pancreatic ribonuclease: the crystal structure of three noncovalent dimeric mutants. *Biopolymers.* 91:1029–1037.
36. Di Donato, A., V. Cafaro, …, G. D'Alessio. 1995. Hints on the evolutionary design of a dimeric RNase with special bioactions. *Protein Sci.* 4:1470–1477.
37. Chakrabartty, A., J. A. Schellman, and R. L. Baldwin. 1991. Large differences in the helix propensities of alanine and glycine. *Nature.* 351:586–588.